Band spectra of rectangular graph superlattices

P. Exner
Nuclear Physics Institute, Academy of Sciences, 25068 Řež near Prague, Czech Republic
and Doppler Institute, Czech Technical University, Břehová 7, 11519 Prague, Czech Republic

R. Gawlista
Lehrstuhl Theoretische Physik I, Fakultät für Physik, Ruhr-Universität Bochum, 44780 Bochum-Querenburg, Germany
(Received 28 July 1995)

We consider rectangular graph superlattices of sides l_1, l_2 with the wave-function coupling at the junctions either of the δ type, when they are continuous and the sum of their derivatives is proportional to the common value at the junction with a coupling constant α, or the δ'_s type with the roles of functions and derivatives reversed; the latter corresponds to the situations where the junctions are realized by complicated geometric scatterers. We show that the band spectra have a hidden fractal structure with respect to the ratio $\theta := l_1/l_2$. If the latter is an irrational badly approximable by rationals, δ lattices have no gaps in the weak-coupling case. We show that there is a quantization for the asymptotic critical values of α at which new gap series open, and explain it in terms of number-theoretic properties of θ. We also show how the irregularity is manifested in terms of Fermi-surface dependence on energy, and possible localization properties under influence of an external electric field.

I. INTRODUCTION

The advent of new technologies that made possible fabrication of semiconductor quantum wires and other tiny structures opened a new chapter in solid-state physics as well as ways to many potentially useful devices. At the same time, this development has an impact on the quantum theory itself, which may not be so spectacular but is by no means less important. The point is that by investigating various ''tailored'' systems one is able to study—both theoretically and experimentally—interesting and sometimes unsuspected effects ''hidden'' in the basic equations of quantum mechanics.

An example is represented by irregular spectral properties due to incommensurability of certain parameters of the system. Such behavior is known to occur, e.g., for two-dimensional lattice electrons in a constant magnetic field.[1–5] In this paper we discuss similar effects that can be observed *without the presence of an external field* in certain graph superlattices.

Before we shall describe the model, a few words should be said about the simplification it involves. A real quantum wire is a complicated many-body system; even if we suppose that it has an ideal crystallic structure, we may describe it as an electron duct at most in a certain range of energies where the profile of the conduction band is reasonably flat. Neglecting the lateral size of the wire, i.e., assuming that the propagating electrons remain in a single transverse mode, is another approximation. It can be justified in thin wires, not only by practical experience, but also by rigorous arguments[6] showing that the intermode coupling involves a dynamical (p-space) tunneling, and therefore it diminishes exponentially with the decreasing wire thickness.

Although the replacement of a quantum wire system by the corresponding graph structure leaves us with a much simpler model, other idealizations may be useful to draw lessons from it. A typical one concerns the global size of the system. As the number of individual cells in a superlattice grows, ''collective effects'' become more important; the question is when they begin to prevail. The larger the superlattice, the more reasonable it is to start from an infinitely extended structure, with the boundary effects considered as a perturbation.

The last introductory remark concerns the question of why various results based on number-theory properties of the parameters represent more than nice mathematics. With a certain exaggeration one can certainly claim that for a mathematician all rationals are the same, while in physics with its finite-resolution experiments it is meaningless to ask whether a measured quantity is irrational or not. Fortunately, differences between number types and between simple and complicated rationals are usually two sides of the same coin.

While theoretically there might be an ultimate difference between the value $\sqrt{2}$ and its close rational approximations, it is manifested over a long scale (in energy, time, etc.); at a shorter scale it is important that the value in question does not coincide with one of simple harmonies. The irrational model thus represents a proper description of the ''disharmonic'' situation. These somehow vague statements can be readily illustrated with the help of the system treated below.

II. DESCRIPTION OF THE MODEL

The configuration space of our model is a two-dimensional lattice graph whose elementary cell is a rectangle of sides l_1, l_2 (cf. Fig. 1). If no external field is applied, the motion of electrons on graph links is free. Since the choice of the energy scale will play no role in the following, we choose atomic units, $\hbar^2/2m^* = 1$, for the sake of simplicity; hence if the wave function ψ is supported in the interior of a single graph link, the Hamiltonian changes it into $-\psi''$.

The nontrivial part of the problem concerns, of course, the

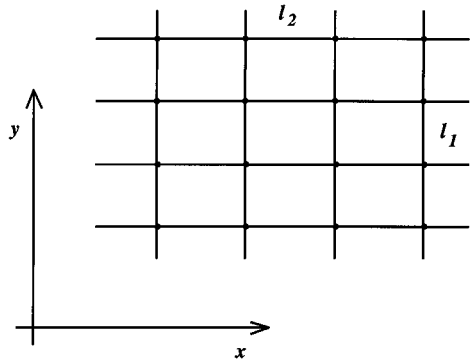

FIG. 1. A rectangular lattice.

behavior at the junctions. The wave functions must be coupled there in such a way that the probability flow is preserved; in mathematical terms that is equivalent to the claim that the Hamiltonian is a self-adjoint operator. This has been known for quite a long time: Schrödinger operators on graphs appeared in quantum mechanics for the first time in connection with the free-electron model of organic molecules,[7] and in recent years interest in them has been revived.[8–16]

The requirement of probability-flow conservation does not specify the coupling uniquely: it can be satisfied, e.g., if the wave functions are continuous at all vertices and their derivatives satisfy there the conditions

$$\sum_j \psi_j'(x_m) = \alpha_m \psi(x_m), \tag{1}$$

where m is the vertex number, the derivatives are taken in the same direction (conventionally outward), the sum runs over all links entering this vertex, $\psi(x_m)$ is the common value of the functions ψ_j there, and the real numbers α_m are coupling constants characterizing the junctions. For the sake of brevity, we shall refer to (1) as the *δ coupling*; the name is motivated by the fact that in the simplest case of just two links this is just the δ interaction on a line.[2]

A choice of the coupling should, of course, be obtained by deriving the graph model from a more realistic description, in which the configuration space consists of a system of coupled tubes. Though a heuristic argument showing that for an ideal starlike junction the conditions (1) with $\alpha_m = 0$ might be the optimal choice was given more than four decades ago,[7] and it is natural to expect that nonzero coupling constants could correspond to the local deformation of the junction region, impurities, or the influence of external fields—in short, *imperfect contacts*—no convincing answer is known up to now.

Moreover, the coupling (1) is not the only possible coupling: for a junction of N links there is in general an N^2 parameter family of self-adjoint operators that act as the free Hamiltonian outside the branching points. A method to construct such operators and some particular classes of them was discussed in detail in Ref. 14. In distinction to (1), the ''additional'' couplings have wave functions *discontinuous* at the vertex, i.e., the limits for at least one pair of links differ mutually there.

This feature is not automatically disqualifying. It was shown in Ref. 10 that the so-called δ' interaction[17] represents a reasonable (if idealized) model for a complicated geometric scatterer, in which instead by a point contact two half lines are joined by numerous short ''wires.'' Moreover, this result extends to junctions with any number of links;[13] the most natural counterpart to (1) appears to be the so-called δ_s' *interaction*, which requires the wave-function *derivatives* to be continuous, $\psi_1'(x_m) = \cdots = \psi_N'(x_m) =: \psi'(x_m)$, and

$$\sum_j \psi_j(x_m) = \beta_m \psi'(x_m) \tag{2}$$

for some β_m. The ''coupling constants'' β_m here measure, roughly speaking, the *total length* of the wires that constitute the geometric scatterer; for a more detailed discussion we refer to Ref. 13.

In what follows we shall be concerned with rectangular lattices in which the coupling at each junction is the same and belongs to one of the above-described types; for the sake of brevity we shall refer to them as the δ and δ_s' lattices, respectively. In a sense, such lattices represent a generalization of the classical Kronig-Penney (KP) model and its δ' modification[2] to higher dimensions.[18]

III. GENERAL PROPERTIES OF THE SPECTRA

Before proceeding further let us recall some results about the spectra of the considered lattice Hamiltonians derived in Ref. 13.

A. δ lattices

By assumption, a δ lattice is a periodic system in both directions. Performing the Bloch analysis, we arrive at the band condition[19]

$$\frac{\cos\vartheta_1 l_1 - \cos k l_1}{\sin k l_1} + \frac{\cos\vartheta_2 l_2 - \cos k l_2}{\sin k l_2} - \frac{\alpha}{2k} = 0. \tag{3}$$

Although an analytic solution can be written in the trivial case only, the condition (3) nevertheless allows one to draw many conclusions about the spectrum. Let us rewrite it in the form

$$\frac{\alpha}{2k} = \sum_{j=1}^{2} \frac{v_j - \cos k l_j}{\sin k l_j};$$

if the quasimomentum components ϑ_j, $j = 1,2$, run though the Brillouin zone, the ranges of the parameters $v_j := \cos\vartheta_j l_j$ cover the interval $[-1,1]$. It is easy to see that for a fixed k, the maximum of the right side equals

$$F_+(k) := \sum_{j=1}^{2} \tan\left(\frac{k l_j}{2} - \frac{\pi}{2}\left[\frac{k l_j}{\pi}\right]\right),$$

where the square bracket denotes conventionally the integer part, and the minimum, $F_-(k)$, is given by a similar formula with tan replaced by $-\cot$. It is clear from here that the gaps of the δ-lattice spectrum with a coupling constant α on the positive part of the energy axis are determined by the condition

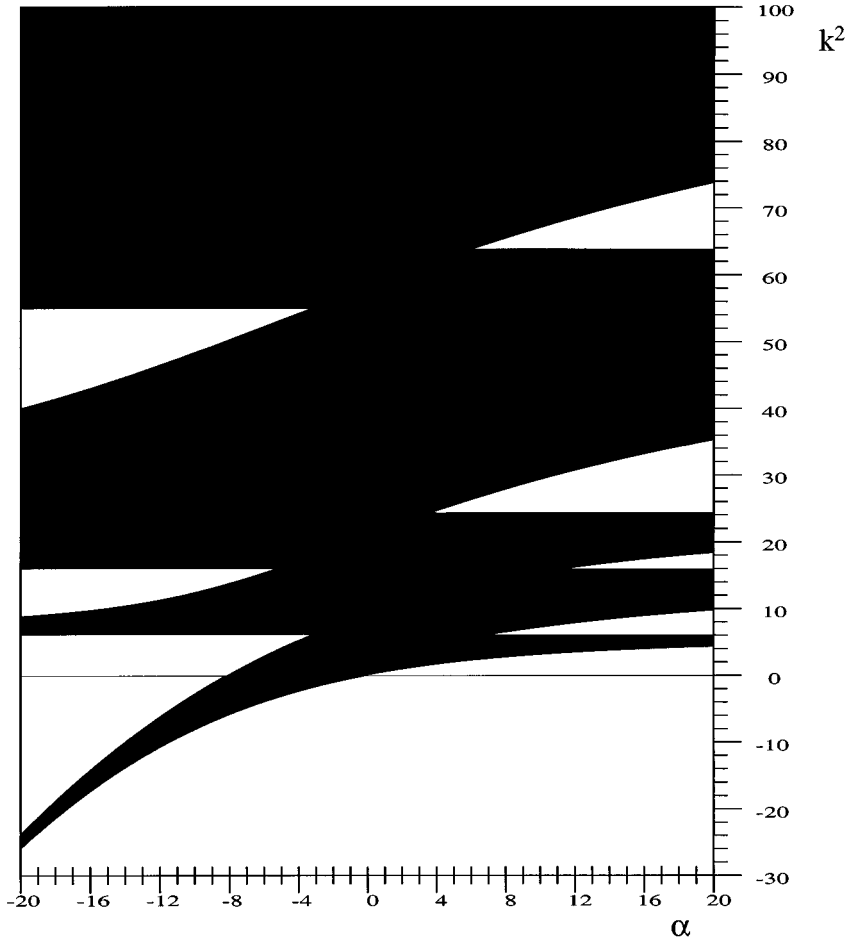

FIG. 2. The golden-mean δ lattice spectrum as a function of the coupling constant.

$$\pm\frac{\alpha}{2k} > \pm F_{\pm}(k) \tag{4}$$

for $\pm\alpha>0$, respectively. The negative part of the spectrum is obtained analogously by comparing $\alpha/2\kappa$ with the extremum values of the function $iF_{\pm}(i\kappa)$. Simple consequences of the condition (4) are the following:

(a1) The spectrum has a band structure; it coincides with the positive half line $[0,\infty)$ if and only if $\alpha=0$.

(a2) If $\alpha>0$, each upper band end is a square of some $k_n:=\pi n/l_1$ or $\tilde{k}_m:=\pi m/l_2$, where n,m are integers. Similarly, for $\alpha<0$ each lower band end, starting from the second one, equals k_n^2 or $\tilde{k}_m^2$.

(a3) The lowest band threshold is positive for $\alpha>0$ and negative if $\alpha>0$; in the case $\alpha<-4(l_1^{-1}+l_2^{-1})$ the whole first band is negative, and the second one starts at $(\pi/L)^2$, where $L:=\max(l_1,l_2)$.

(a4) The positive bands shrink with increasing $|\alpha|$.

(a5) Each gap is contained in the intersection of a pair of gaps of the Kronig-Penney model with the coupling constant α and spacings l_1 and l_2, respectively.

(a6) All gaps above the threshold are finite. If there are infinitely many of them, their widths are asymptotically bounded by $2|\alpha|(l_1+l_2)^{-1}+O(r^{-1})$, where r is the gap number.

Most of these results have a natural meaning. In particular, (a5) shows that transport properties of the lattice are better than a combination of its one-dimensional projections. Notice that the Kronig-Penney spectral condition[2] can be cast into the form (a3) with a single trigonometric expression on the left-hand side (lhs). If an energy value is contained in a Kronig-Penney band in one of the directions, it is trivially also in a band of the lattice Hamiltonian, the other factor being annulated by choosing $\theta_j=k$. The converse is not true, of course: the condition (a3) may be satisfied even if none of the factors can be annulated separately. The directions in which the electron is able to ''dribble'' through the lattice will be seen in Sec. VI below.

Less trivial is the irregular dependence of the spectrum on the rectangle-side ratio $\theta:=l_2/l_1$ coming from the existence of competing periods in $F_{\pm}(k)$. It appears that it is not only rationality or irrationality of θ that matters, but also the type of irrationality plays a role. In this respect, the situation is similar to the almost Mathieu equation mentioned in the Introduction.

Let us recall some elementary facts from the number theory.[20] An irrational number θ is *badly approximable* by rationals if there is a positive δ such that $|q\theta-p|>\delta q^{-1}$ holds for all integers p,q. There are uncountably many such numbers; nevertheless, they are rather exceptional in the sense that they form a zero-measure set. Its complement to the set of all irrationals consists of numbers that we shall call *Last admissible*.[5] A convenient way to characterize these number types is through their unique continued-fraction rep-

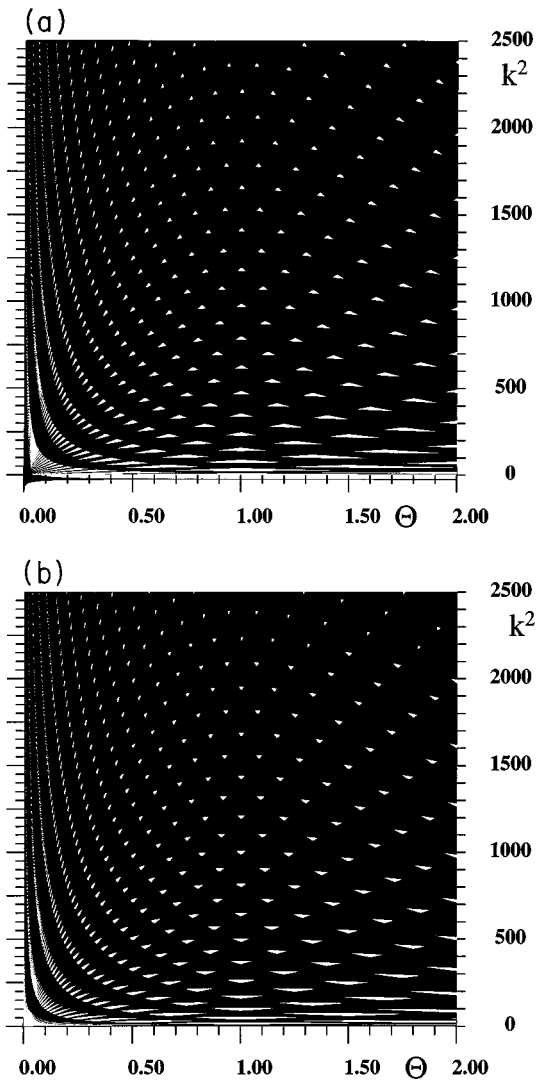

FIG. 3. (a) δ-lattice spectrum as a function of the ratio θ for $\alpha=-20$. (b) δ-lattice spectrum as a function of the ratio θ for $\alpha=20$.

resentations: θ is badly approximable if and only if the infinite sequence of integer coefficients in this representation is bounded, and Last admissible otherwise. Needless to say, rationals have finitely many nonzero coefficients.

If θ is irrational, the right-hand side of (4) is never zero; the existence of gaps requires then that there is a subsequence of local minima that tends sufficiently fast to zero. In this way we were able in Ref. 13 to prove the following results:

(a7) For a badly approximable θ there is $\alpha_0>0$ such that for $|\alpha|<\alpha_0$ the spectrum has no gaps above the threshold.
(a8) The number of gaps is infinite for any θ provided $|\alpha|L>5^{-1/2}\pi^2$; recall that $L:=\max(l_1,l_2)$.
(a9) If θ is rational or Last admissible, there are infinitely many gaps for any $\alpha\neq 0$.

The worst irrational in this sense is the golden mean $\theta=\frac{1}{2}(1+\sqrt{5})$, which has the continued-fraction representation $\theta=[1,1,\ldots]$. In this case the sufficient condition for the existence of infinitely many gaps is necessary at the same time and coincides with the critical value of the claim (7): $|\alpha_0|L$ is $\pi^2(5\theta)^{-1/2}=3.4699,\ldots$; more about that will be said in Sec. V below.

B. δ'_s lattices

Replacing the δ coupling by the boundary conditions (2), one can derive the band equation in this case:[13]

$$\frac{\cos\vartheta_1 l_1+\cos kl_1}{\sin kl_1}+\frac{\cos\vartheta_2 l_2+\cos kl_2}{\sin kl_2}-\frac{\beta k}{2}=0; \qquad (5)$$

the same argument as above then shows that spectral *bands* of the δ'_s lattice with a coupling constant β are determined by the inequalities

$$\mp F_{\mp}(k)\geq\pm\frac{\beta k}{2} \qquad (6)$$

for $\pm\beta>0$ and $k>0$, and an analogous relation for the negative part.

The structure of the spectrum is now different; the condition (6) allows one to make the following conclusions:

(b1) The spectrum equals $[0,\infty)$ if and only if $\beta=0$; otherwise there are infinitely many gaps.
(b2) If $\beta>0$, the lower end of each band coincides with some k_n^2 or $\tilde{k}_m^2$, where n,m are integers. The same is true for $\beta<0$ and the upper band ends, with the exception of the first one.
(b3) The lowest band threshold is positive for $\beta>0$ and negative if $\beta<0$; in the case $-l_1-l_2<\beta<0$ the whole first band is negative, and the second one starts at zero.
(b4) The positive bands shrink with increasing $|\beta|$.
(b5) Each gap is contained in the intersection of a pair of δ' Kronig-Penney gaps[2] with the coupling constant β and spacings l_1 and l_2, respectively.

Instead of the asymptotic behavior (a6) of δ lattices, we have a slightly more complicated result. If a band high in the spectrum is well separated, its width Δ_r is the same as in the δ' Kronig-Penney model, $\Delta_r=8/\beta l_j+O(r^{-1})$. Furthermore, if θ is rational and two bands intersect, $k_n=\tilde{k}_m$ for some n,m, we have a similar expression with l_j^{-1} replaced by $l_1^{-}+l_2^{-1}$. It may happen, however, that k_n and $\tilde{k}_m$ are not identical but close to each other, so that they still produce a single band. Then the bandwidth is enhanced; the effect is most profound just before the band splits. Using the condition (5), it is straightforward to estimate the factor of enhancement by conspiracy of bands:[13] asymptotically we have the relation

$$\frac{8}{\beta L}+O(r^{-1})<\Delta_r<\frac{32}{3\beta}(l_1^{-1}+l_2^{-1})+O(r^{-1}). \qquad (7)$$

This brief survey shows, in particular, that despite the generally irregular pattern, the spectra of δ and δ'_s lattices inherit the main feature of their Kronig-Penney analogues, namely that they are dominated asymptotically by bands and gaps, respectively, at high energies. At the same time, the above listed results leave many questions open about the actual form of these spectra and related quantities. In the following sections we are going to answer some of them.

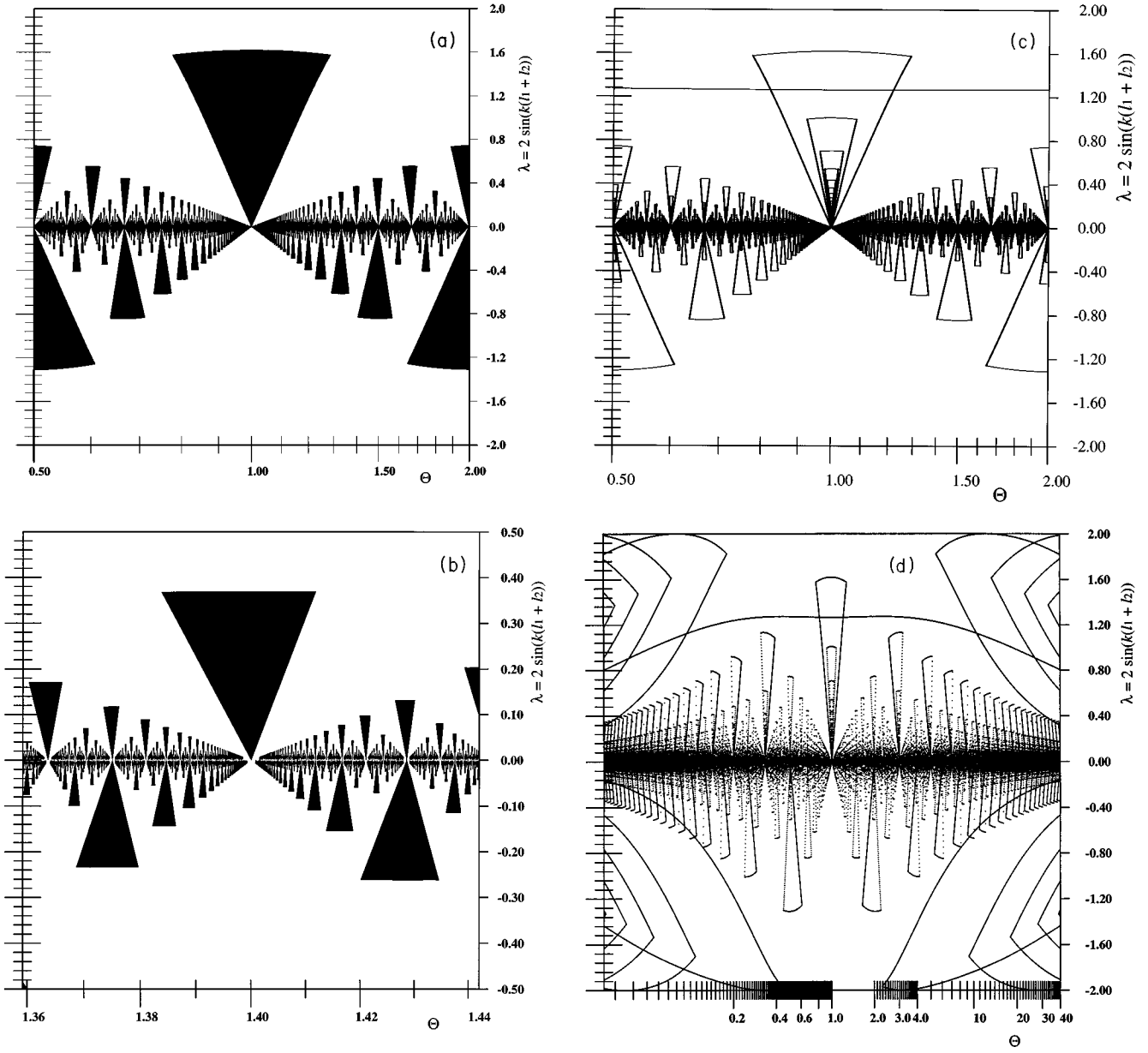

FIG. 4. (a) The folded δ-lattice spectrum as a function of θ (with the θ axis logarithmically scaled): The regions with at least one gap; the lowest one, (1,1), is deleted. (b) The folded δ-lattice spectrum as a function of θ (with the θ axis logarithmically scaled): An inset of the previous picture. (c) The folded δ-lattice spectrum as a function of θ (with the θ axis logarithmically scaled): The plot of gap edges in the same scale as (a). (d) The folded δ-lattice spectrum as a function of θ (with the θ axis logarithmically scaled): Gap edges in a wider scale, with several lowest of the $(n_1,1)$ and $(1,n_2)$ gaps shown.

IV. δ-LATTICE SPECTRA

The form (4) of the gap condition makes it possible to find the δ-lattice spectra numerically in dependence on parameters of the model; the results are shown in Figs. 2 and 3. The effect of competing periods is obvious: while a square lattice has a familiar Kronig-Penney spectrum shape[2] with the halved coupling constant as expected from the gap condition, in the general case the gap pattern is irregular.

The dependence of spectral bands on the ratio θ shows clearly that the gaps are contained in view of (a5) in the intersections of KP gaps. The latter can be numbered by an integer n such that $\pi n l_j^{-1}$ is the lower (upper) gap end for $\pm\alpha>0$, respectively (with $n=0$ referring to the region below the bottom of the spectrum[2]). This allows us to label the gaps of a δ lattice naturally by a pair (n_1,n_2) with the integers n_j tagging the KP gaps. Notice also that due to (a2) the actual gaps occupy the lower part of the allowed region if $\alpha>0$, and the upper one for $\alpha<0$. Asymptotically each intersection is of a parallelepiped form and the actual gap part represents a diagonal cut of it, which conforms with (a6).

Although the θ plots look rather regular, they contain a hidden irregular pattern that is revealed if the spectrum is properly folded. A way to do that is suggested by a relation between the present model and the theory of multidimensional Jacobi matrices[21] by which $\lambda=2\sin[k(l_1+l_2)]$ is the natural ''folded'' energy variable, the above-introduced gap labeling then has a direct relation to that of Ref. 3. The folded spectrum is illustrated on Fig. 4; we plot λ against $\ln\theta$

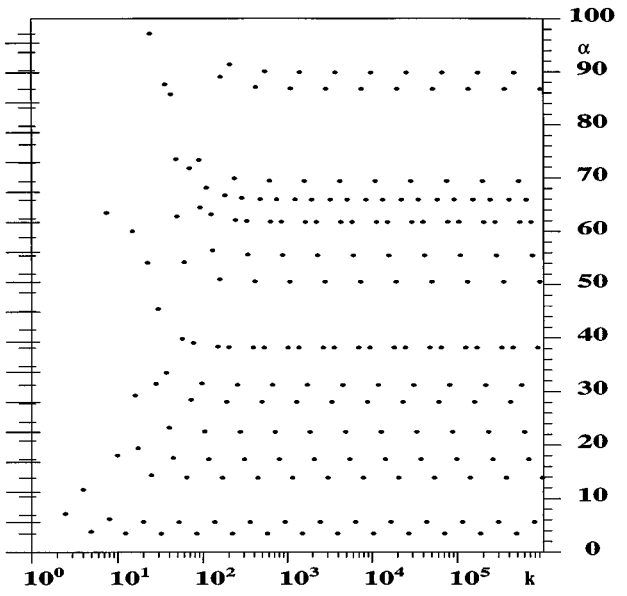

FIG. 5. Critical coupling constants for the golden-mean δ lattice.

to show the symmetry with respect to the exchange of the basic cell sides. All the gaps close, of course, and the multiplicity is infinite, but it changes in a fractal way[22] as is seen when we plot the regions where the original spectrum has at least one gap. For the sake of illustration we delete here the ''regular'' (1,1) gap which produces a concave strip covering a part of the upper half of the picture. Similar ''nonfractal'' contributions come from the gaps $(n_1,1)$ and $(1,n_2)$ with $n_j \geq 2$, which enter the picture at sufficiently large $|\ln\theta|$. Each gap of the fractal structure ''contains'' an infinite series of embedded gaps as can be seen if we plot just the gap edges; for instance, the central element (2,2) of the picture is, in fact, a sequence $(2,2)\supset(3,3)\supset(4,4)\supset\cdots$.

V. CRITICAL COUPLING CONSTANTS

Due to (a7), the spectrum may contain no gaps if the ratio θ is badly approximable and the coupling is weak enough. To get a better understanding of how the number-theoretic properties of the parameter imply this result, let us discuss in more detail the ''worst'' case of the golden-mean lattice, $\theta = \frac{1}{2}(1+\sqrt{5})$.

Suppose that the coupling constant grows from the zero value. The condition (4) shows that a new gap opens whenever the hyperbolic graph of the function on the lhs crosses a local minimum of the function $F_+(\,)$. These critical values of the coupling together with the corresponding momenta are shown on Fig. 5. One can make from here several conclusions:

(i) Gaps open in series. The asymptotic behavior is clearly visible and the critical points approach the asymptotic value from above; hence a new infinite series of gaps opens ''from above'' once the coupling constant crosses the next critical value.

(ii) The critical points are extremely sparse; we see that the patterns are practically equidistant in the logarithmic scale. This is a nice illustration of the fact that θ is badly approximable: to obtain the next close approximation to it we have to use integers that are roughly twice as large as their predecessors.

(iii) The asymptotic critical values are quantized; they appear at multiples of the two basic values $\pi^2/l\sqrt{5}\,\theta^{\pm 1/2}$, where $l := \sqrt{l_1 l_2}$. However, not every multiple yields a critical value: in both series the same sequence of integers repeats, namely,

$$1,4,5,9,11,16,19,20,25,\ldots\ . \tag{8}$$

Let us attempt to explain this quantization rule. Recall that the golden mean is approximated by ratios of successive Fibonacci numbers,[17] $\theta = \lim_{n\to\infty} u_{n+1}u_n^{-1}$, where the u_n satisfy the recursive relation $u_{n+1}=u_n+u_{n-1}$ and assume the values $1,2,3,5,8,13,21,\ldots$ for $n=1,2,\ldots$. In the continued-fraction representation the nth approximant equals $\theta_n=[1,\ldots 1,0,\ldots]$ with $n+1$ nonzero coefficients.

Let us ''spoil'' the approximation by choosing instead the sequence of $\theta_n^N := [1,\ldots,1,N,0,\ldots]$ with a fixed positive integer N preceded by n ones. This can be alternatively written as $q_{n+1}q_n^{-1}$, where $q_n := Nu_n + u_{n-1}$, so that

$$q_n^2\left(\theta - \frac{q_{n+1}}{q_n}\right) = \left[N\frac{\theta^n-(-\theta)^{-n}}{\sqrt{5}} + \frac{\theta^{n-1}-(-\theta)^{-n+1}}{\sqrt{5}}\right] \times(-\theta)^{-n+1}\left(1-\frac{N}{\theta}\right) \to (-1)^n\frac{1+N-N^2}{\sqrt{5}}$$

as $n\to\infty$. The asymptotic threshold values thus are

$$\frac{\pi^2}{l\sqrt{5}}\,\theta^{\pm 1/2}|N^2-N-1|,$$

which yields the integer multiples $1,5,11,19,29,41,\ldots$ explaining part of the values (8) but not all of them. The missing numbers can be obtained if we consider a more general approximation to the golden mean,

$$\theta_n^{A,B} := \frac{Au_{n+2}+Bu_{n+1}}{Au_{n+1}+Bu_n} \tag{9}$$

for some positive A,B. The numerical factor in the above limit is then replaced by $|A^2-B^2-AB|$, so the complete sequence (8) is obtained when A,B run through positive integers. What is important is that A,B here need *not* be relatively prime. This can be seen directly: it is clear from (4) that replacing approximation sequences $\{q_n\}$, $\{p_n\}$ by $\{Mq_n\}$, $\{Mp_n\}$ means that the corresponding local minima of $F_+(k)$ are enhanced by a factor that tends to M as $n\to\infty$. These are compared with $\alpha/2\kappa$ at the minima, which is *divided* by M, so the asymptotic critical value of the modified sequence is multiplied by M^2. In the logarithmic scale the x coordinates referring to the modified sequence are just shifted by a multiple of $\ln M$; this is also seen in Fig. 5.

In this way, we are able to explain how the successive infinite gap series open in the spectrum as the coupling constant α increases.

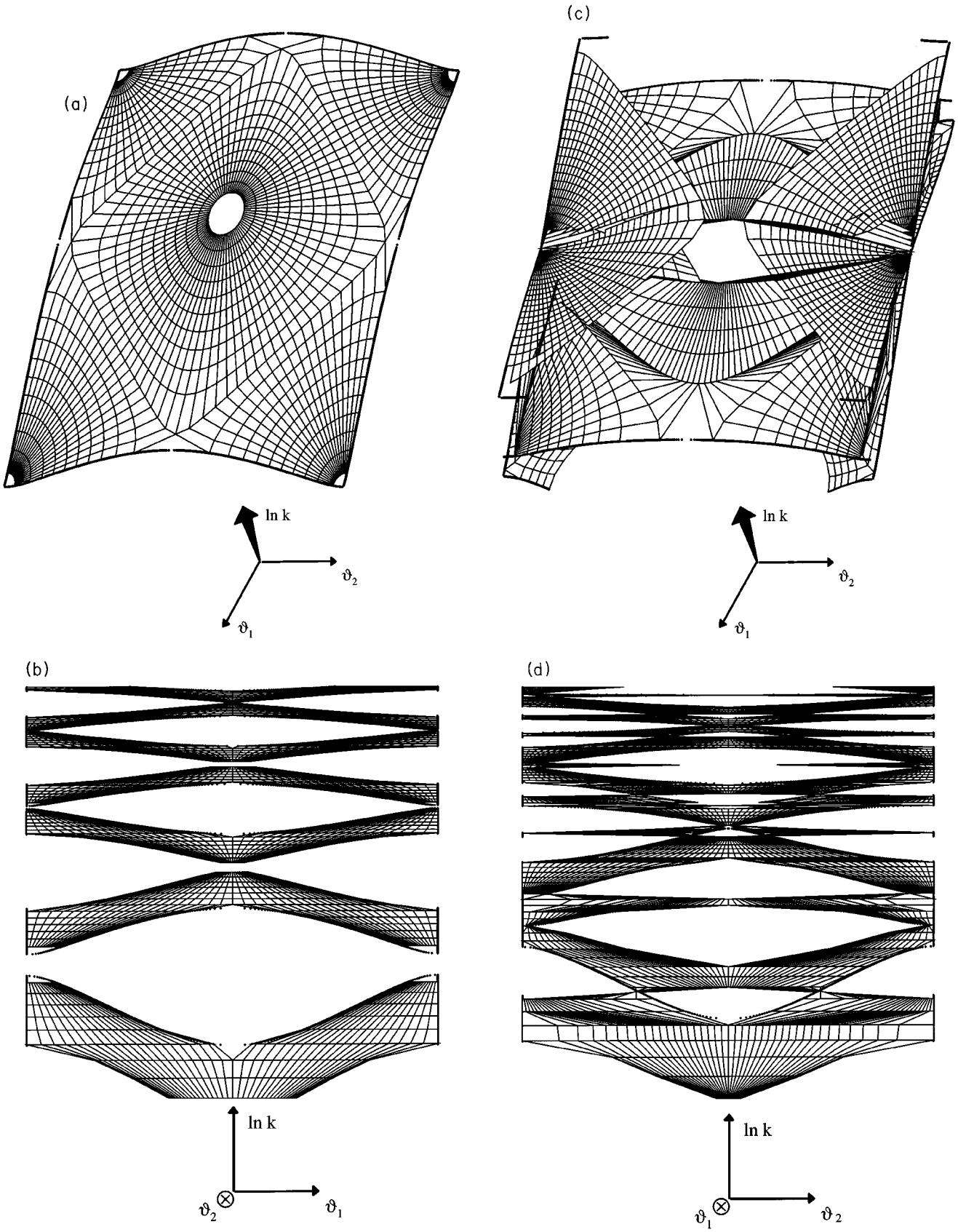

FIG. 6. (a) Fermi surfaces for different energies for the second band of a square δ lattice. (b) Fermi surfaces for different energies, the ''side view'' for the same lattice and the logarithmic scale of energy, $1 \leqslant k \leqslant 21$. (c) Fermi surfaces for different energies for the second band of a golden-mean δ lattice. (d) Fermi surfaces for different energies, the ''side view'' for the same lattice and the logarithmic scale of energy, $1 \leqslant k \leqslant 21$.

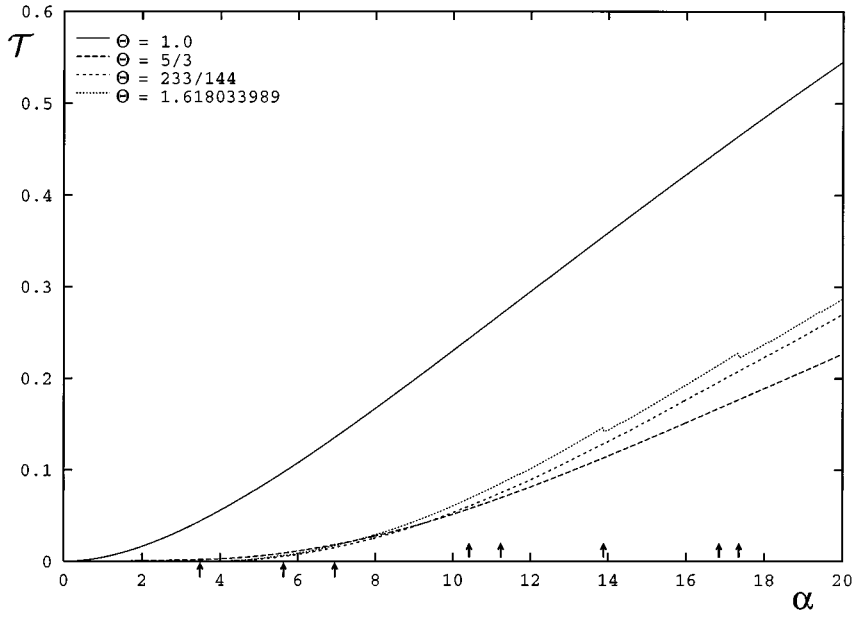

FIG. 7. The quantity $\tau(\theta,\alpha)$ as a function of the coupling constant for $\theta=1$, $\frac{5}{3}$, $\frac{233}{144}$, and the golden mean. The arrows mark distinguishable gap openings.

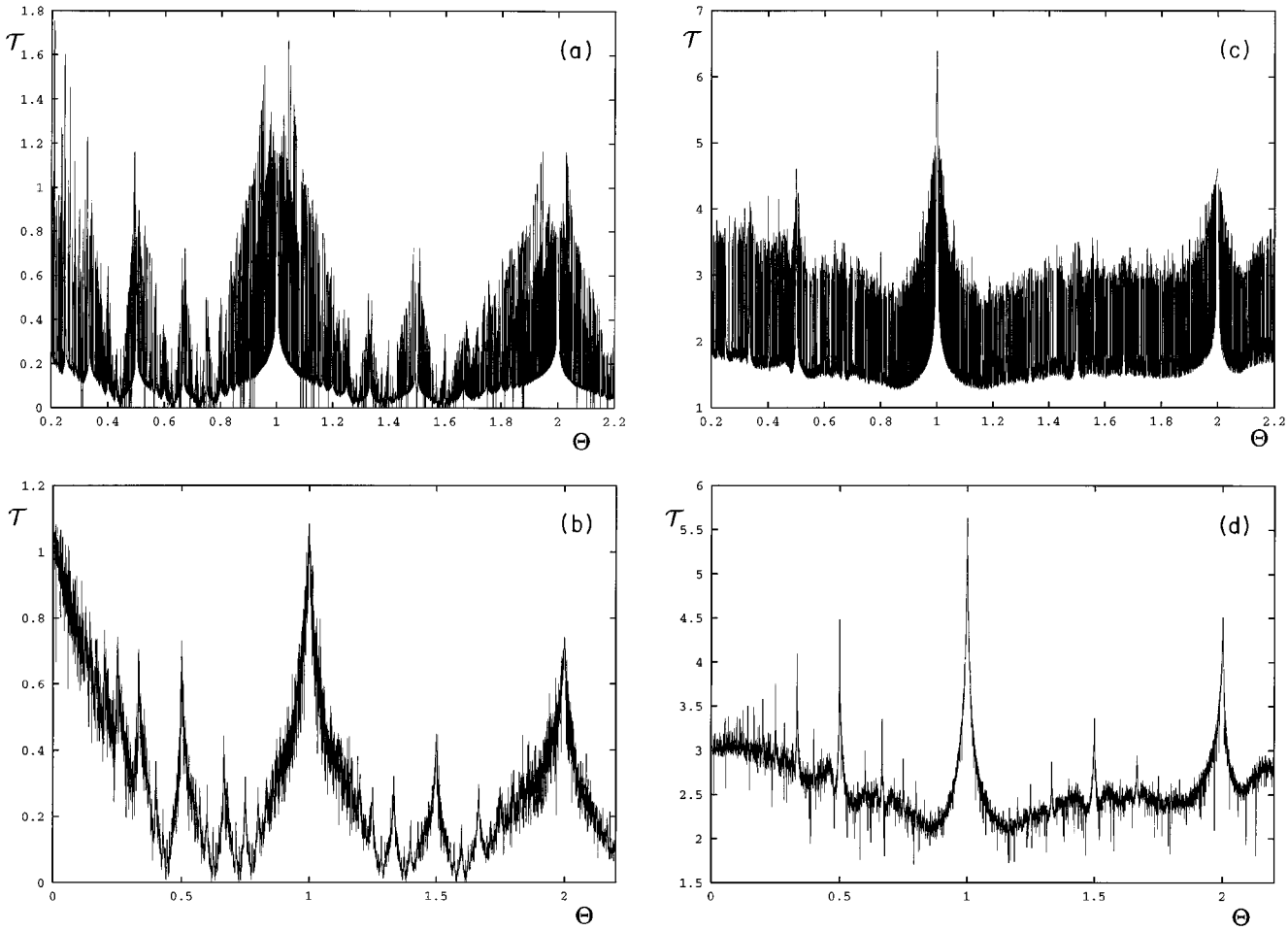

FIG. 8. (a) The quantity $\tau(\theta,\alpha)$ as a function of θ. Plot for $\alpha=3.4699$ over rational values of θ. (b) The quantity $\tau(\theta,\alpha)$ as a function of θ. Plot for $\alpha=3.4699$ with θ being random identically distributed numbers. (c) The quantity $\tau(\theta,\alpha)$ as a function of θ. Plot for $\alpha=20$ over rational values of θ. (d) The quantity $\tau(\theta,\alpha)$ as a function of θ. Plot for $\alpha=20$ with θ being random identically distributed numbers.

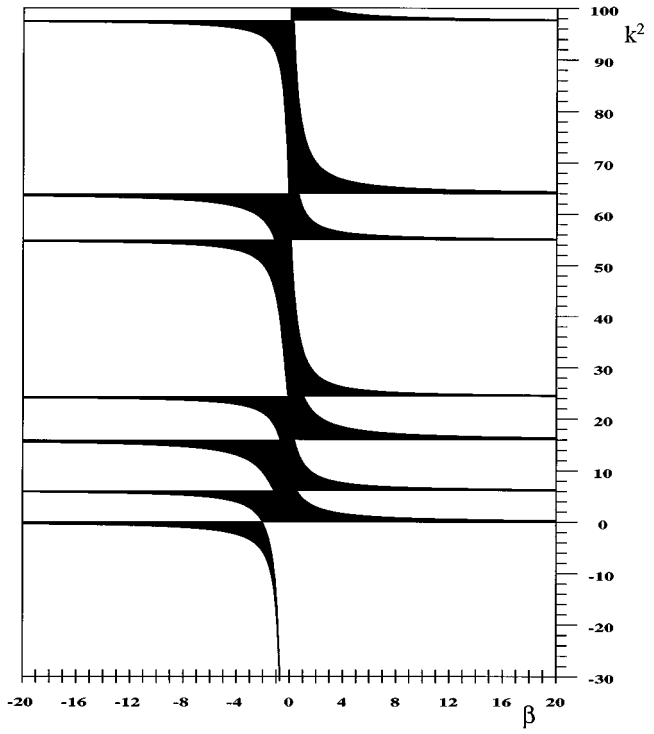

FIG. 9. The coupling constant plot for the δ_s'-lattice spectrum in the golden-mean case.

VI. FERMI SURFACES

The above results do not exhaust all possible irregularities of the model in question. The fact that a given energy value is contained in a spectral band tells us nothing about the directions in which the electron may propagate. To this end we have to find what are the allowed values of the quasimomentum, i.e., to determine the Fermi surface. As mentioned above, the Brillouin zone is the rectangle

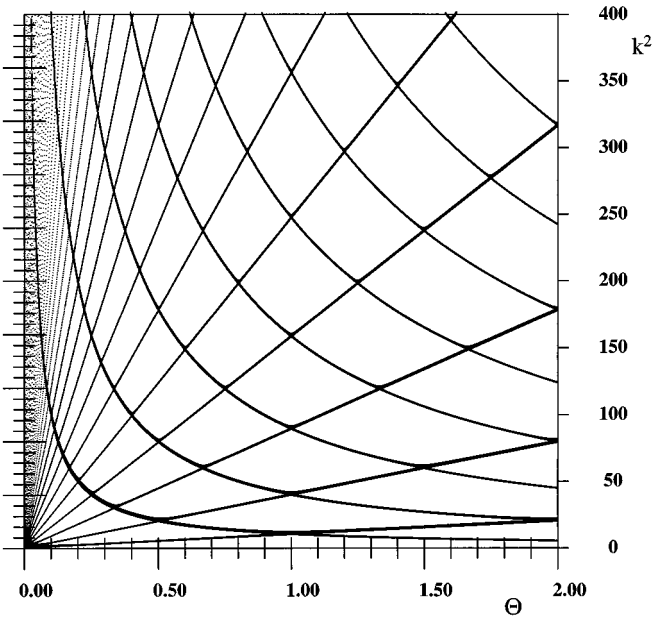

FIG. 10. The δ_s'-lattice spectrum as a function of the θ for $\beta=5$.

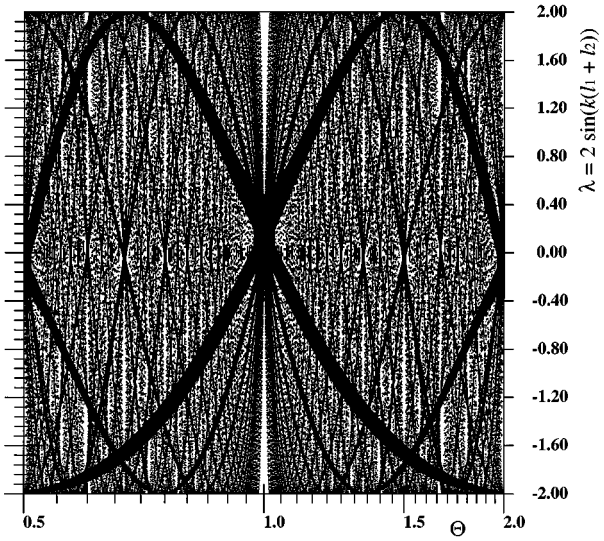

FIG. 11. The folded δ_s'-lattice spectrum as a function of θ (with the θ axis logarithmically scaled) for $\beta=20$. The value of momentum is restricted to $k\leqslant 100$.

$$\mathscr{B}:=\left[-\frac{\pi}{l_1},\frac{\pi}{l_1}\right)\times\left[-\frac{\pi}{l_2},\frac{\pi}{l_2}\right), \tag{10}$$

and the Fermi surface is a one-dimensional submanifold in it. Since it has a fourfold symmetry due to the invariance of the condition (3) with respect to the interchanges $\vartheta_j\leftrightarrow-\vartheta_j$, it is sufficient to consider a quadrant of $\mathscr{B}$. The change of variables $v_j:=\cos\vartheta_j l_j$ maps it on the square $[-1,1]\times[-1,1]$; the band condition becomes at that

$$\frac{v_1}{\sin kl_1}+\frac{v_2}{\sin kl_2}=\frac{\alpha}{2k}+\cot kl_1+\cot kl_2$$

describing a line segment that crosses the square provided k corresponds to a point in a spectral band. Passing back to the quasimomentum coordinates we see that the Fermi surface can have one of several standard shapes.

On the other hand, the way in which the surface changes as a function of the Fermi energy depends substantially on the ratio θ. This is illustrated in Fig. 6 where we plot the two-dimensional manifolds spanned by the Fermi surface as the energy increases; to see the change over a larger range of energies we choose for the latter a logarithmic scale. We see that for a square lattice the surface ''evolution'' produces a regular pattern of switching ''caps'' reminiscent of the corresponding quantity for the one-dimensional Kronig-Penney model,[2] while in the golden-mean case the dependence is highly irregular.

Another lesson from the dependence of Fermi surfaces on energy concerns the character of the spectrum. To avoid spectral singularities, the solution $k=k(\theta_1,\theta_2)$ of Eq. (3) has to be smooth with local extrema at discrete points only. The lhs of (3), which we denote as $D(k,\theta_1,\theta_2)$, is certainly smooth in all variables away of the points $kl_j=n\pi$, and

$$\frac{\partial D}{\partial k}(k,\theta_1,\theta_2)=\frac{l_1}{\sin^2/kl_1}+\frac{l_2}{\sin^2/kl_2}+\frac{\alpha}{2k^2}\neq 0$$

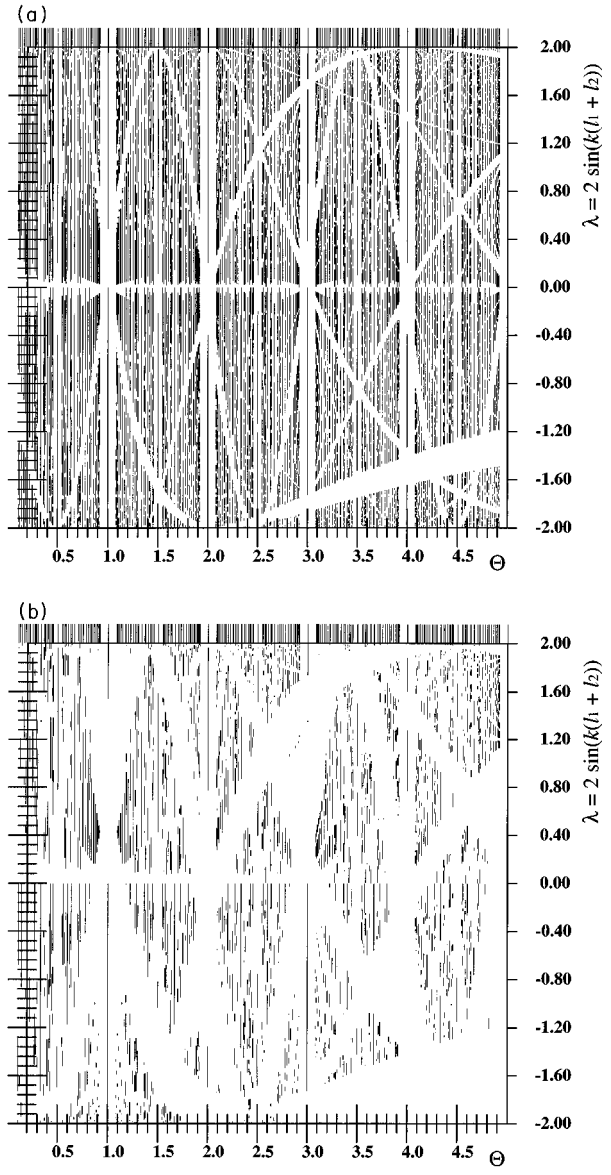

FIG. 12. (a) Folded-spectrum gaps (black) for rational approximations to the golden mean, $\beta=20$. (b) Folded-spectrum gaps (black) for rational approximations to the golden mean, $\beta=5$.

holds there, with a possible exception of a discrete set of points for $\alpha<0$. Hence $k(\theta_1,\theta_2)$ is smooth by the implicit-function theorem and

$$\frac{\partial k}{\partial \theta_j}(\theta_1,\theta_2)=-l_j\frac{\sin\theta_j l_j}{\sin k l_j}\left(\frac{\partial D}{\partial k}(k,\theta_1,\theta_2)\right)^{-1},$$

which may be simultaneously zero only if $\theta_j l_j=\pm\pi$, $j=1,2$. This means that stationary points of $k(\theta_1,\theta_2)$ are only at the center of the Brillouin zone or at its cornerpoints; we conclude that

(a10) The δ lattice spectrum in the bands is absolutely continuous.

This is not just a mathematical statement; it tells us that the transport properties of electrons in the allowed energy windows are ''normal.''

VII. EXTERNAL FIELDS

Adding an external field, even a simple one like a linear potential, makes the problem much more difficult, and we are not able to present more than several heuristic observations. Recall that the problem is far from being understood even in the one-dimensional case. It has been demonstrated recently that an array of δ' interactions has no absolutely continuous spectrum when an electric field is applied;[10,23] this result extends to a wide class of background potentials.[24] Moreover, one may conjecture that the spectrum of δ' Wannier-Stark ladders depends substantially on the slope of the potential being pure point and nowhere dense if the latter is rational, and covering the whole real axis otherwise.[23]

The case of a periodic δ array is more difficult and only partial results are known,[25–27] though it is generally believed that a phase transition occurs in this case with the spectrum being pure point at weak fields and continuous if the field is strong.[26] The critical field value can be conjectured to be $F_{\rm crit}\approx\alpha^2/4a$, where a is the array spacing and F the field intensity, using the argument of Ref. 26, which is based on estimating the tunneling probability through the family of tilted spectral gaps.[28] The result is intuitively appealing because it compares two values having an established meaning: the energy step Fa with the bound-state energy $\alpha^2/4$ of a single δ well. However, the argument neglects the fact that in some tilted gaps the other (exponentially growing) solution for the classically forbidden region may play a role, and therefore it is not *a priori* clear whether this is the correct answer.

Applying the same tilted-band picture to the two-dimensional situation, one may conjecture that in a δ'_s lattice whose spectrum is dominated by the gaps at high energies, an external electric field is likely to produce a localization in the field direction; in other words, electrons would be able to move at most in the direction *perpendicular* to the field.

In the δ lattice case the situation is more complicated. Even if a Berezhkovski-Ovchinnikov-type (BO) argument[26] could be justified, it will yield now only a lower bound to the power with which the solution to the Schrödinger equation decays, because a gap-width counting disregards the fact that at some energies belonging to a band a propagation is possible in certain directions only. With this reservation in mind, let us compute the expression that is a two-dimensional analogue of the BO power: it equals $(\pi/16F)\mathscr{T}(\theta,\alpha)$ with

$$\mathscr{T}(\theta,\alpha):=\lim_{n\to\infty}\frac{1}{\ln n}\sum_{m=1}^{n}\frac{|\delta_m|^2}{k_m}, \tag{11}$$

where $\delta_m\equiv\delta_m(\theta,\alpha)$ are the corresponding gap widths.

Due to the results of Sec. IV, namely, the property (a4), the sum in (11) is monotonously increasing as a function of $|\alpha|$, the growth being roughly quadratic. The same behavior is expected for $\mathscr{T}(\theta,\alpha)$ though for a badly approximable θ the existence of the thresholds discussed in Sec. V may lead to local deformations of this dependence around the threshold values of α; this is illustrated on Fig. 7.

On the other hand, let us fix the coupling constant at two

values, $\alpha=3.4699,\ldots$ for which we know that $\mathscr{T}(\theta,\alpha)$ has a zero, and $\alpha=20$, and plot the θ dependence (Fig. 8). Simple harmonic values of the ratio produce well-pronounced peaks; hence the corresponding lattices are expected to exhibit better localization properties when an electric field is applied. On the other hand, $\mathscr{T}(p/q,\alpha)$ may depend substantially on the integers p,q involved. To illustrate the difference we compute first this quantity for $p,q=1,2,3,\ldots$ with $q\leqslant 150$, and after that we plot $\mathscr{T}(\theta,\alpha)$ with random identically distributed θ values; the latter are almost surely ''typical,'' i.e., irrational.

VIII. δ_s'-LATTICE SPECTRA

Let us finally check what the spectra of δ_s' lattices look like. They can be found with the help of the condition (6); in the same way as above, we can also check that

(b6) the δ_s' lattice spectrum in the bands is absolutely continuous.

Figure 9 shows the dependence of spectral bands on β, again for the golden-mean case, $\theta=\frac{1}{2}(1+\sqrt{2})$; we see that the pattern has *globally* the same behavior as the δ' Kronig-Penney spectrum.[2] On the other hand the θ plot (Fig. 10) illustrates the properties (b2) and (b5); the latter can be again used to label the gaps. Moreover, we see clearly the enhancement due to conspiracy of bands—cf. (7).

As in the δ situation, the spectrum may be folded into $2\sin[k(l_1+l_2)]$; this is shown on Fig. 11. We have deleted here again the lowest ''regular'' band, which can be done unambiguously if $|\ln\theta|$ is small enough. In this case the folded spectrum leaves, in general, some gaps open, but it may happen at rational values of θ only. Indeed, it is not difficult to check that for an irrational θ spectrum the folded spectrum has a full measure. It is sufficient to notice that all the points $(\pi n/l)\theta^{\pm 1/2}$ with both signs are contained in a band, either as its lower edge (upper edge for $\beta<0$) or an internal point. The corresponding values of λ are then $2\sin[\pi n(1+\theta^{\pm 1})]$; they cover the interval $[-2,2]$ due to the basic result of the ergodic theory.[29] On the other hand, for rational θ some gaps remain open; this is illustrated in Fig. 12.

IX. CONCLUSIONS

We have demonstrated irregular properties of rectangular δ and δ_s' lattices with incommensurate sides, as they are manifested in the form of their spectra, critical coupling-constant values, dependence of the Fermi surface on the Fermi energy, and possibly in localization properties under influence of external fields. These features are expected to play a dominating role in the behavior of finite but large enough graph superlattices. It is also natural to conjecture that similar geometrically induced spectral properties will be seen in superlattices in which the basic cell has another form.

One lesson drawn from the present considerations concerns the validity of the so-called *Bethe-Sommerfeld conjecture* by which the number of gaps in periodic systems of dimensions two or higher is finite. This was proven by Skriganov[30] for Schrödinger operators with nice potentials, and it is known to be valid also for some systems with δ interactions.[2] We have seen that the conjecture may not be valid if the periodic structure is singular enough: the golden-mean δ lattice has, depending on the value of the coupling constant α, either infinitely many gaps or *none at all*.

ACKNOWLEDGMENTS

The work was done during the visits of P.E. at the Institut für Mathematik, Ruhr-Universität Bochum and R.G. at the Nuclear Physics Institute, Czech Academy of Sciences; the authors express their gratitude to the hosts. The research has been partially supported by Grants AS No. 148409 and GACR No. 202-93-1314, by the European Union Project ERB-CIPA-3510-CT-920704/704 and by the ''Deutsche Forschungsgemeinschaft'' (SFB 237).

[1] The literature about this subject is huge; let us just mention the classical papers: P. G. Harper, Proc. R. Soc. London Ser. A **68**, 874 (1955); D. R. Hofstadter, Phys. Rev. B **14**, 2239 (1976). For a more complete bibliography to this problem, which is usually referred to as the ''almost Mathieu equation,'' see Ref. 2, Sec. III.2.5 or Ref. 3; recent mathematical results are discussed, e.g., in Refs. 4 and 5.

[2] S. Albeverio, F. Gesztesy, R. Høegh-Krohn, and H. Holden, *Solvable Models in Quantum Mechanics* (Springer-Verlag, Heidelberg, 1988).

[3] J. Bellissard, in *Number Theory and Physics*, edited by M. Waldschmidt *et al.* (Springer, Heidelberg, 1992), pp. 538–630.

[4] M. A. Shubin, Commun. Math. Phys. **164**, 259 (1994).

[5] Y. Last, Commun. Math. Phys. **164**, 421 (1994).

[6] P. Duclos, P. Exner, and P. Šťovíček, Ann. Inst. H. Poincaré Phys. Théor. **62**, 81 (1995).

[7] K. Ruedenberg and C. W. Scherr, J. Chem. Phys. **21**, 1565 (1953).

[8] V. M. Adamyan, Oper. Theory Adv. Appl. **59**, 1 (1992).

[9] Y. Avishai and J. M. Luck, Phys. Rev. B **45**, 1074 (1992).

[10] J. E. Avron, P. Exner, and Y. Last, Phys. Rev. Lett. **72**, 896 (1994).

[11] J. E. Avron, A. Raveh, and B. Zur, Rev. Mod. Phys. **60**, 873 (1988).

[12] W. Bulla and T. Trenckler, J. Math. Phys. **31**, 1157 (1990).

[13] P. Exner, Phys. Rev. Lett. **74**, 3503 (1995); J. Phys. A (to be published).

[14] P. Exner and P. Šeba, Rep. Math. Phys. **28**, 7 (1989).

[15] J. Gratus, C. J. Lambert, S. J. Robinson, and R. W. Tucker, J. Phys. A **27**, 6881 (1994).

[16] N. I. Gerasimenko and B. S. Pavlov, Sov. J. Theor. Math. Phys. **74**, 345 (1988).

[17] A single-center δ' interaction is defined by the requirement of the wave-function derivative continuity together with the condition $\psi(0+)-\psi(0-)=\beta\psi'(0)$ for some ''coupling constant'' β. A thorough discussion of its properties can be found in Ref. 2.

[18] Considerations of the present paper allow a straightforward extension to graph lattices in dimension $d\geqslant 3$.

[19] The condition (3) was obtained in Ref. 6 for $\alpha=0$ and extended to the nonzero-coupling case in Ref. 12. These authors pursued other goals, however, and therefore restricted themselves to writ-

ing down the solution in the trivial situation.

[20] G. H. Hardy and E. M. Wright, *An Introduction to the Theory of Numbers* (Oxford University Press, New York, 1979); W. M. Schmidt, *Diophantine Approximations and Diophantine Equations*, Lecture Notes in Mathematics Vol. 1467 (Springer-Verlag, Berlin, 1991).

[21] P. Exner, Ann. Inst. H. Poincaré Phys. Theor. (to be published).

[22] We use this term in a somewhat loose sense without insisting that the folded-gap pattern is exactly self-similar.

[23] M. Maioli and A. Sacchetti, J. Phys. A **28**, 1101 (1995).

[24] P. Exner, J. Math. Phys. **36**, 4561 (1995).

[25] F. Bentosela and V. Grecchi, Commun. Math. Phys. **142**, 169 (1991), and references therein.

[26] A. M. Berezhkovski and A. A. Ovchinnikov, Fiz. Tverd Tela (Leningrad) **18**, 3273 (1976) [Sov. Phys. Solid State **18**, 1908 (1976)].

[27] P. Ao, Phys. Rev. B **41**, 3998 (1990).

[28] To get the stated result from this argument, a numerical factor describing the tunneling through a single gap must be properly evaluated as pointed out by F. Bentosela.

[29] I. P. Cornfeld, S. V. Fomin, and Ya. G. Sinai, *Ergodic Theory* (Springer, New York, 1982), Theorem 7.2.1.

[30] M. M. Skriganov, Sov. Math. Doklady **20**, 956 (1979); Invent. Math. **80**, 107 (1985); see also Yu. E. Karpeshina, Proc. Steklov Math. Inst. **3**, 109 (1991).